Synchronized PWM Control of Asymmetrical Dual-Inverter Fed Open-End Winding Traction Drive

G. Grandi[1], V. Oleschuk[2], F. Dragonas[1]

[1]University of Bologna, Italy
[2]Power Engineering Institute of the Academy of Sciences of Moldova

Abstract — **Space-vector-based synchronized PWM algorithms have been applied to the control of a dual-inverter fed open-end winding induction motor drive supplied by two isolated dc sources with non-equal voltages. It has been shown that algorithms of synchronized PWM provide continuous phase voltage symmetry for any ratio (integral or fractional) of switching frequency to fundamental frequency of the inverters and also for any ratio between the two dc source voltage levels of these systems. Phase voltage spectra of open-end winding drives for both continuous and discontinuous schemes of synchronized PWM do not contain even harmonics and sub-harmonics during the whole control range, including the zone of overmodulation which is especially important for the medium and high-power traction systems.**

I. INTRODUCTION

Some of the most interesting and promising power converter topologies are cascaded (dual) converters, which utilize two standard three-phase voltage source inverters [1]-[8]. The structure of ac motor drives based on cascaded inverters is realised by splitting the neutral connection of the induction motor and connecting each end of the phase windings to a two-level inverter. In this way, cascaded converters are capable of producing voltages which are identical to those of three- and four-level converters [3]-[9].

Dual-inverter fed open-end winding motor drives have some advantages such as redundancy of the space-vector combinations and the absence of neutral point fluctuations. In particular, a dual-inverter scheme has a total of 64 switch combinations distributed over 19 space-vector locations compared to 27 switch combinations distributed over the same number of locations for a typical three-level neutral-point-clamped inverter [3]-[5] Among perspective fields of application of open-end winding drives there can be traction and propulsion systems with increased power rating.

It is known that for high power/high current drives symmetry of the output voltage waveforms of the converters is necessary in order to eliminate undesirable current and voltage sub-harmonics [10]-[12]. In order to avoid asynchronism of standard schemes of space-vector modulation, a novel method of synchronized PWM has been proposed, developed and applied to different topologies of converters, drives, and renewable energy systems [13]-[18].

In this paper, both continuous and discontinuous schemes of space-vector-based synchronized PWM, including specialized schemes of synchronized PWM, have been applied to the control of an asymmetrical dual-inverter fed open-end winding drive supplied by two isolated dc sources with non-equal voltages.

II. BASIC TOPOLOGY OF ASYMMETRICAL DUAL-INVERTER FED OPEN-END WINDING MOTOR DRIVE

Fig. 1 presents the basic structure of a dual inverter-fed open-end winding induction motor drive, where INVERTER-1 and INVERTER-2 are standard three-phase voltage source inverters. Two isolated dc sources with different (asymmetrical) voltages (V_{dc} and $V_{dc}/2$) are being used. Consequently, the phase voltage of the system results in four-level waveforms [9].

Fig. 2 shows the switching state vectors of the two inverters, which provide avoidance of overcharging dc-link capacitors of INVERTER-2 which operates at a lower dc-voltage [9]. The switch state sequences (voltage vectors) of phases ***abc*** for each inverter is expressed in the conventional form. In particular, for INVERTER-1: **1** – 100; **2** – 110; **3** – 010; **4** –011; **5** – 001; **6** – 101, **0** – 000, **7** - 111 (1 - switch-on state, 0 – switch-off state); in the same way for INVERTER-2: **1'** – 1'0'0'; **2'** – 1'1'0'; **3'** – 0'1'0'; **4'** –0'1'1'; **5'** – 0'0'1'; **6'** – 1'0'1'; **0'** – 0'0'0'; **7'**– 1'1'1', where 1' - switch-on state of the switches, and 0' – switch-off state.

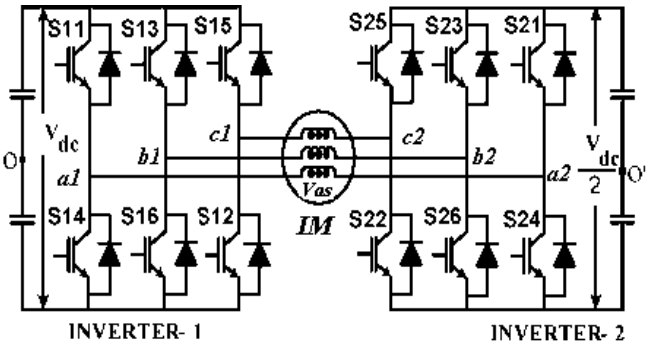

Fig. 1. Asymmetrical dual-inverter fed drive with two dc-sources.

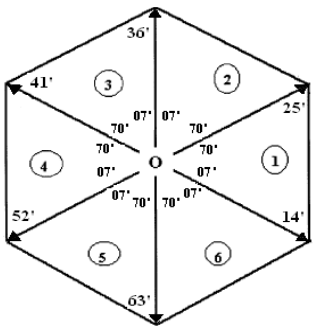

Fig. 2. Voltage space-vector combinations, providing avoidance of overcharging of the dc-source capacitors with lower voltage.

III. Peculiarities and Features of the Method of Synchronized Space-Vector Modulation

Algorithms of synchronized space-vector-based PWM for drive converters provide a continuous symmetry of phase voltage waveforms and can be successfully used for the control of each inverter in a dual-inverter system.

Figs. 3 - 4 present the switching state sequences of a standard three-phase inverter inside the interval 0° - 90°. Two basic versions of space-vector PWM (Fig. 3 – continuous PWM (CPWM), and Fig. 4 – discontinuous PWM with 30°-non-switching intervals (DPWM)) [13] are schematically illustrated.

The upper trace in Figs. 3 – 4 is the switching state sequences (in accordance to conventional designation [13]), while the middle ones correspond to the pole voltages of a standard three-phase inverter. The lower trace shows the corresponding quarter-wave of the line-to-line output voltage of the inverter. Signals β_k represent the total switch-on duration inside the switching cycles τ, while signals γ_k are generated in the centers of the corresponding β interval. Widths of notches λ_k represent the duration of zero states.

One of the basic ideas of the proposed PWM method is the continuous synchronization of the position of all central β_1-signals inside each 60°-clock-interval (fixing the positions of the β_1-signals in the center), with further symmetrical generation of other active β- and γ-signals, together with the corresponding notches, around each β_1-signal.

Also in the output curve, special signals λ' (λ_5 for CPWM, λ_4 for DPWM in Figs. 3-4) with neighboring β' (β_5 for CPWM, β_4 for DPWM) are formed at the clock-points (0°, 60°, 120°...). They are simultaneously reduced until close to zero value at boundary frequencies F_i, providing a continuous adjustment of voltage with smoothly changing pulse ratio. F_i is calculated in a general form as a function of duration of sub-cycles τ in accordance with (1), and the neighboring $F_{i\text{-}1}$ - from (2). Here, index i is equal to the number of notches inside half of the 60°-clock-intervals and is determined from (3), where a fraction is rounded off to the nearest higher integer:

$$F_i = 1/[6(2i - K_1)\tau] \quad (1)$$

$$F_{i-1} = 1/[6(2i - K_2)\tau] \quad (2)$$

$$i = (1/6F + K_1\tau)/2\tau, \quad (3)$$

where K_1=1, K_2=3 for CPWM, K_1=1.5, K_2=3.5 for DPWM.

Equations (4) - (9) present a set of control functions for the determination of the duration, in absolute values (seconds), of all the control signals of the three-phase inverters with synchronized PWM for both linear modulation and over-modulation control regimes [13]:

For j = 2, ... i-1:

$$\beta_j = \beta_1 \cos[(j - 1 - K_3)\pi K_{ov1}] \quad (4)$$

$$\gamma_j = \beta_{i-j+1}\{0.5 - 0.87\tan[(i - j - 0.25)\tau]\}K_{ov2} \quad (5)$$

$$\beta_i = \beta'' = \beta_1 \cos[(i - 1.25)\pi K_{ov1}]K_s \quad (6)$$

$$\gamma_1 = \beta''\{0.5 - 0.87\tan[(i - 2.25)\tau + (\beta_{i-1} + \beta_i + \lambda_{i-1})/2]\}K_s K_{ov2} \quad (7)$$

$$\lambda_j = \tau - (\beta_j + \beta_{j+1})/2 \quad (8)$$

$$\lambda_i = \lambda' = (\tau - \beta'')K_{ov1}K_s, \quad (9)$$

where: $\beta_1 = 1.1\tau m$ (m is modulation index) if m<0.907, and $\beta_1 = \tau$ if m>0.907; $K_s = [1 - (F - F_i)/(F_{i-1} - F_i)]$, $K_{ov1} = 1$ until F_{ov1}=0.907F_m, and $K_{ov1} = [1 - (F - F_{ov1})/(F_{ov2} - F_{ov1})]$ between F_{ov1} and $F_{ov2} = 0.952F_m$; $K_{ov2} = 1$ until F_{ov2}, and $K_{ov2} = [1 - (F - F_{ov2})/(F_m - F_{ov2})]$ in the zone between F_{ov2} and F_m; K_3=0.25 for DPWM, and K_3=0 for CPWM.

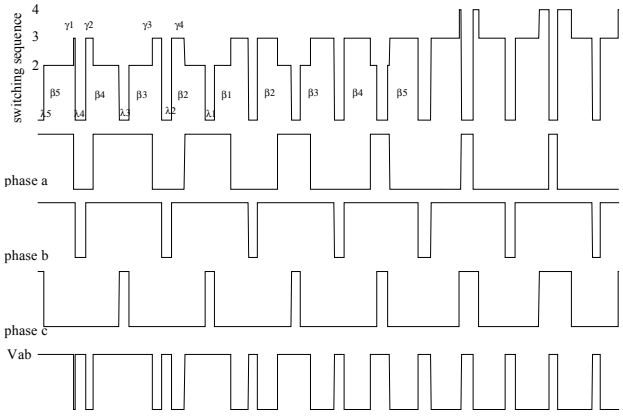

Fig. 3. Switching state sequence, pole voltages V_a, V_b, V_c, and line voltage V_{ab} of inverter with continuous PWM (CPWM).

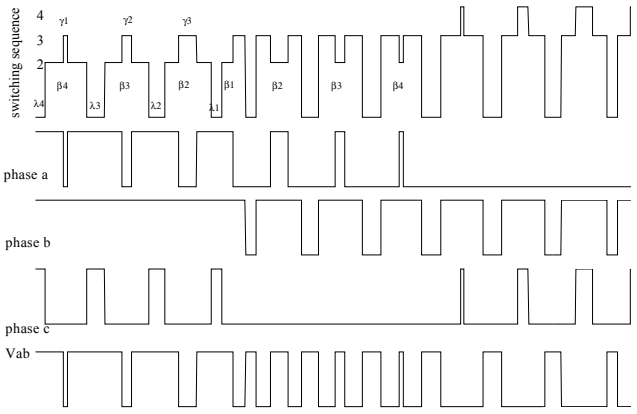

Fig. 4. Switching state sequence, pole voltages V_a, V_b, V_c, and line voltage V_{ab} of inverter with discontinuous PWM (30^0-non-switching intervals, DPWM).

IV. Algorithms of Synchronized PWM for Control of Asymmetrical Dual-Inverter Fed System

The control of each inverter in a dual-inverter system that relies on algorithms of synchronized PWM, and in accordance with the switching scheme presented in Fig. 2, provides continuous symmetry of phase voltage waveforms during the whole control range of an open-end winding motor drive. In this case the output voltages of the two inverters have an opposite polarity, with an additional phase shift between voltage waveforms which is equal to one half of the switching interval τ (i.e. a sub-cycle equal to 0.5τ) [1].

The phase voltage V_{as} which is the basis of the dual inverter system is calculated in accordance with (10)-(11) [9]:

$$V_0 = 1/3(V_{a1o} - V_{a2o} + V_{b1o} - V_{b2o} + V_{c1o} - V_{c2o}) \quad (10)$$

$$V_{as} = V_{a1o} - V_{a2o} - V_0, \quad (11)$$

where V_{a1o} , V_{b1o} , V_{c1o} , V_{a2o} , V_{b2o} , and V_{c2o} are the corresponding pole voltages of each inverter, V_0 is the zero sequence voltage component in the system.

As an illustration of the control of an asymmetrical dual-inverter system with synchronized PWM and with non-equal dc-source voltages (V_{dc} and $V_{dc}/2$), Figs. 5–8 show the pole voltages V_{a1o} and V_{a2o}, the zero sequence voltage V_0, and the phase voltage V_{as} (with its spectrum) of such a dual-inverter system with continuous (Figs. 5-6) and discontinuous (Figs. 7-8) synchronized PWM, for scalar *V/F=const* control mode. The fundamental and switching frequencies of each inverter (averaged switching frequency for discontinuous PWM) are correspondingly F=39*Hz* and F_s=1*kHz*.

Modulation indexes are m_1=m_2=0.78 and in this case ratio between the switching frequency and fundamental frequency is equal to 1000*Hz*/39*Hz*=25.6. It is clear that the spectra of the presented voltage waveforms do not contain even harmonics or sub-harmonics.

In some cases (some control modes) controlling the respective switching frequencies of the two inverters in a dual inverter system can result in increasing the effectiveness of the power conversion [9], [17]. In particular, for the asymmetrical open-end winding configuration of the analyzed drive system, the lower dc link voltage is half the value of the other dc link voltage and it is possible to proportionately increase the switching frequency of the inverter supplied by the lower dc voltage. Figs. 9-12 present the respective basic phase voltage waveforms and spectra for a system with continuous (Figs. 9-10) and discontinuous (Figs. 11-12) synchronized PWM with different switching frequencies of the two inverters (F_{s1}=1*kHz*, F_{s2}=2*kHz*).

At this point it is necessary to mention that algorithms of synchronized modulation provide symmetry of phase voltage waveforms in dual-inverter configuration systems for any dc voltage ratio between two isolated dc sources (and also for any of the inverters' switching frequencies). As an illustration of this fact, Figs. 13-16 show the basic phase voltage waveforms and spectra for a system with two dc voltages V_{dc2} = 0.7V_{dc1} and scalar *V/F* control mode. The fundamental frequency of the inverters is equal to F=32*Hz* (in this case modulation indexes are m_1=m_2=0.64), and the inverters' switching frequencies are correspondingly F_{s1}=1*kHz* and F_{s2}=1.43*kHz*.

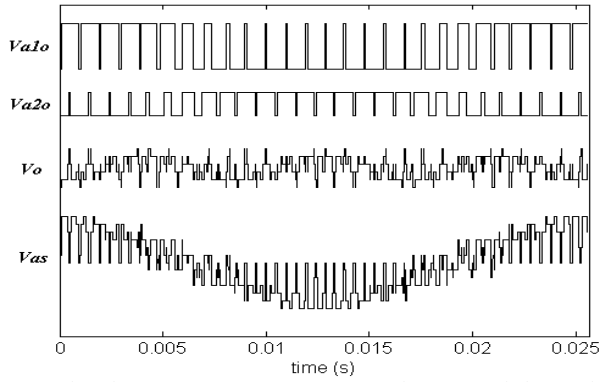

Fig. 5. Pole voltages V_{a1o}, V_{a2o}, zero sequence voltage V_0, and phase voltage V_{as} of dual-inverter fed system with continuous synchronized PWM (F=39*Hz*, F_s=1*kHz*, m_1=m_2=0.78).

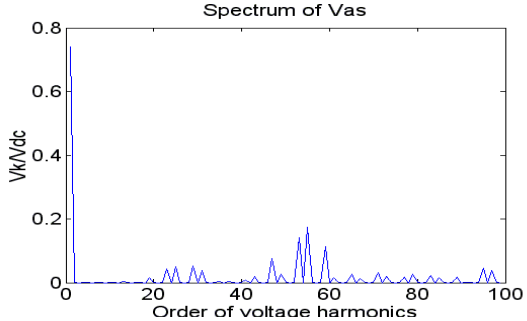

Fig. 6. Spectrum of the phase voltage V_{as} of the system with continuous synchronized PWM (F=39*Hz*, F_s=1*kHz*).

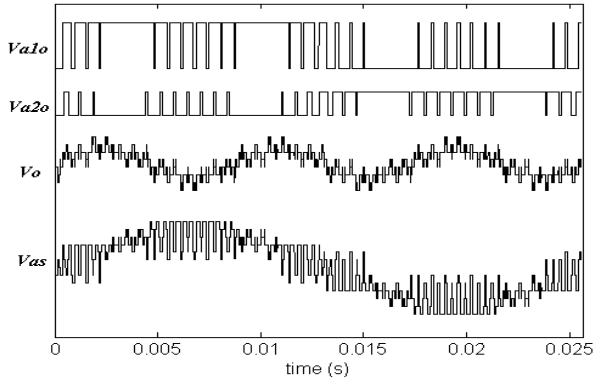

Fig. 7. Pole voltages V_{a1o}, V_{a2o}, zero sequence voltage V_0, and phase voltage V_{as} of dual-inverter fed system with discontinuous synchronized PWM (F=39*Hz*, F_s=1*kHz*, m_1=m_2=0.78).

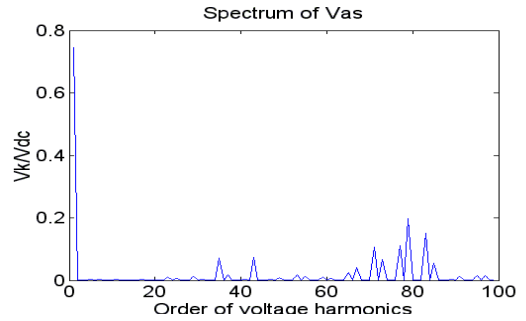

Fig. 8. Spectrum of the phase voltage V_{as} of the system with discontinuous synchronized PWM (F=39*Hz*, F_s=1*kHz*).

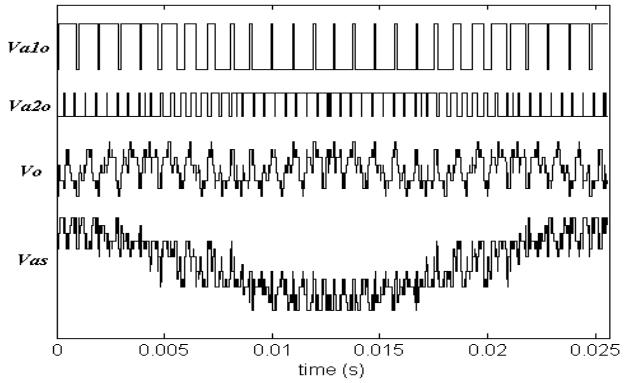

Fig. 9. Pole voltages V_{a1o}, V_{a2o}, zero sequence voltage V_0, and phase voltage V_{as} of dual-inverter fed system with continuous synchronized PWM (F=39Hz, F_{s1}=1kHz, F_{s2}=2kHz , m_1=m_2=0.78).

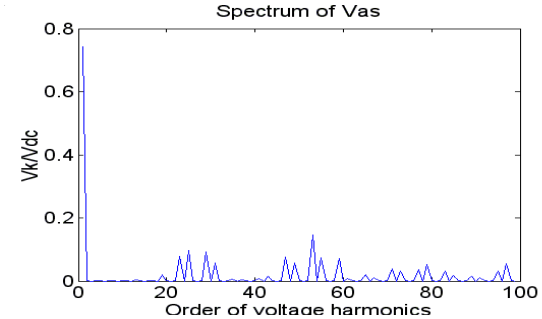

Fig. 10. Spectrum of the phase voltage V_{as} of the system with continuous synchronized PWM (F=39Hz, F_{s1}=1kHz, F_{s2}=2kHz).

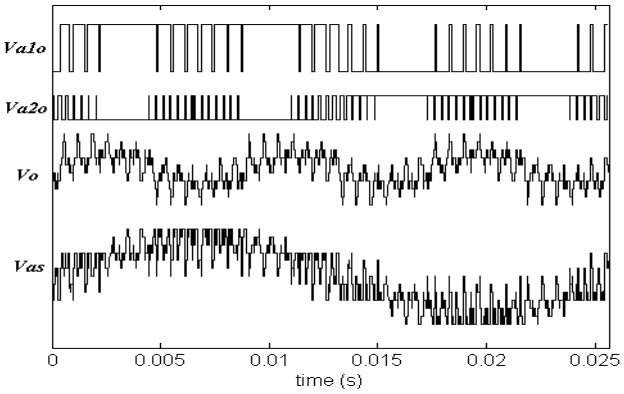

Fig. 11. Pole voltages V_{a1o}, V_{a2o}, zero sequence voltage V_0, and phase voltage V_{as} of dual-inverter fed system with discontinuous synchronized PWM (F=39Hz, F_{s1}=1kHz, F_{s2}=2kHz , m_1=m_2=0.78).

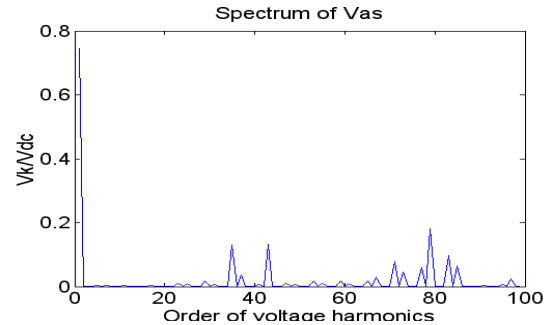

Fig. 12. Spectrum of the phase voltage V_{as} of the system with discontinuous synchronized PWM (F=39Hz, F_{s1}=1kHz, F_{s2}=2kHz).

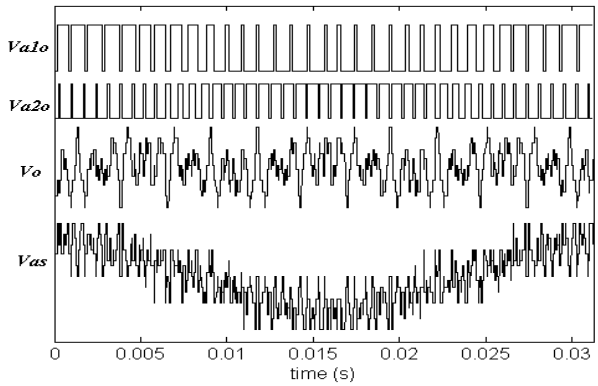

Fig. 13. Pole voltages V_{a1o}, V_{a2o}, zero sequence voltage V_0, and phase voltage V_{as} of dual-inverter fed system with continuous synchronized PWM (F=32Hz, V_{dc2}=0.7V_{dc1}, F_{s1}=1kHz, F_{s2}=1.43kHz , m_1=m_2=0.64).

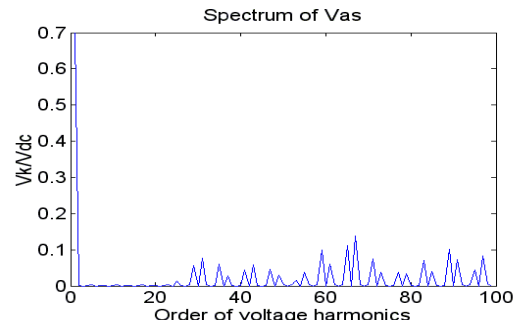

Fig. 14. Spectrum of the phase voltage V_{as} of the system with continuous synchronized PWM (F=32Hz, , V_{dc2}=0.7V_{dc1}, F_{s1}=1kHz, F_{s2}=1.43kHz).

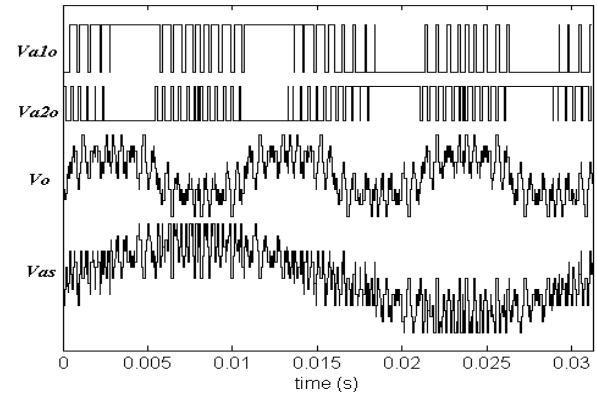

Fig. 15. Pole voltages V_{a1o}, V_{a2o}, zero sequence voltage V_0, and phase voltage V_{as} of dual-inverter fed system with discontinuous synchronized PWM (F=32Hz, V_{dc2}=0.7V_{dc1}, F_{s1}=1kHz, F_{s2}=1.43kHz , m_1=m_2=0.64).

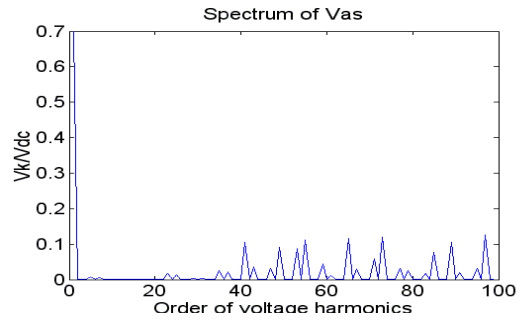

Fig. 16. Spectrum of the phase voltage V_{as} of the system with discontinuous synchronized PWM (F=32Hz,, V_{dc2}=0.7V_{dc1}, F_{s1}=1kHz, F_{s2}=1.43kHz).

Again, spectra of the presented phase voltage waveforms (see Figs. 6, 8, 10, 12, 14, 16) do not contain even harmonics or sub-harmonics for any operating condition of the dual-inverter fed open-end winding motor drive system.

V. Synchronized PWM Control during Overmodulation

This method of synchronized space-vector modulation of dual-inverter systems also provides high quality linear control of the fundamental voltage in the zone of overmodulation. For this particular purpose, the basic control correlations (4)-(9) of the synchronised PWM method include two special overmodulation coefficients K_{ov1} and K_{ov2} [13]. Reference [15] contains a description of the operation of two-level inverters with algorithms of synchronized PWM during overmodulation.

A dual-inverter system (Fig. 1) composed of two inverters with different switching frequencies is taken for example. Figs. 17-18 present the basic phase voltage waveforms and spectrum of such system with discontinuous synchronized PWM (F=47Hz, m_1=m_2=0.94, F_{s1}=1kHz, F_{s2}=2kHz) in the first part of the overmodulation zone.

As an example of the operation in the second part of the overmodulation zone (F=49.5Hz, m_1=m_2=0.99), Figs. 19-22 show the basic phase voltage waveforms and spectrum of the dual-inverter system using discontinuous synchronized PWM with different switching frequencies (Figs. 19-20, F_{s1}=1kHz, F_{s2}=2kHz), and also with equal switching frequencies (Fig. 21-22, F_{s1}=F_{s2}=1kHz).

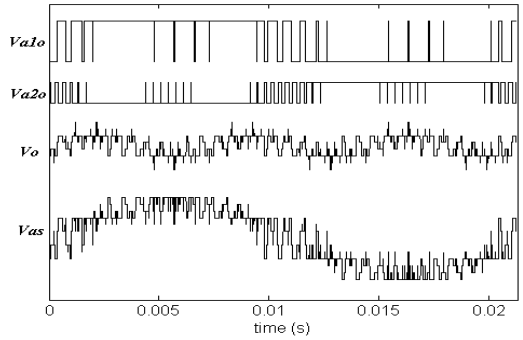

Fig. 17. Pole voltages V_{a1o}, V_{a2o}, zero sequence voltage V_0, and phase voltage V_{as} of dual-inverter fed system with discontinuous synchronized PWM (F=47Hz, V_{dc2}=0.5V_{dc1}, F_{s1}=1kHz, F_{s2}=2kHz , m_1=m_2=0.94).

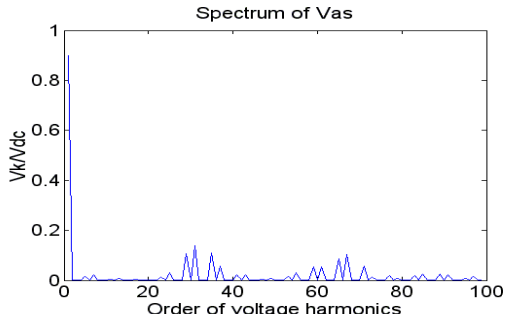

Fig. 18. Spectrum of the phase voltage V_{as} of the system with discontinuous synchronized PWM (F=47Hz, V_{dc2}=0.5V_{dc1}, F_{s1}=1kHz, F_{s2}=2kHz).

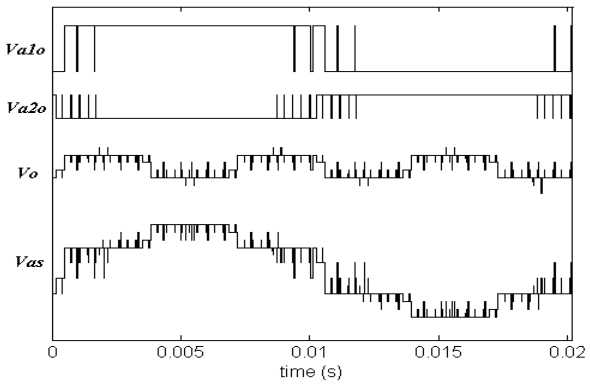

Fig. 19. Pole voltages V_{a1o}, V_{a2o}, zero sequence voltage V_0, and phase voltage V_{as} of dual-inverter fed system with discontinuous synchronized PWM (F=49.5Hz, V_{dc2}=0.5V_{dc1}, F_{s1}=1kHz, F_{s2}=2kHz , m_1=m_2=0.99).

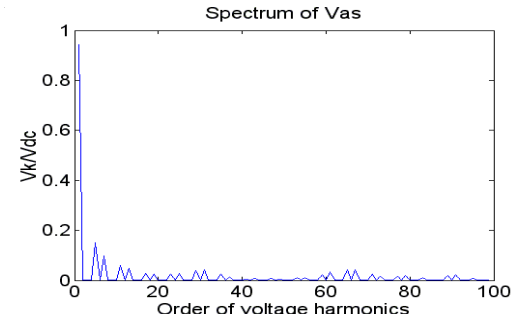

Fig. 20. Spectrum of the phase voltage V_{as} of the system with discontinuous synchronized PWM (F=49.5Hz, V_{dc2}=0.5V_{dc1}, F_{s1}=1kHz, F_{s2}=2kHz).

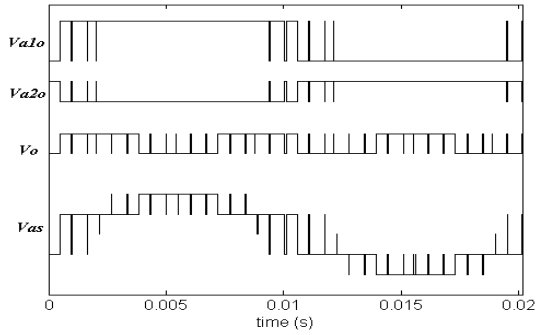

Fig. 21. Pole voltages V_{a1o}, V_{a2o}, zero sequence voltage V_0, and phase voltage V_{as} of dual-inverter fed system with discontinuous synchronized PWM (F=49.5Hz, V_{dc2}=0.5V_{dc1}, F_{s1}=F_{s2}=1kHz , m_1=m_2=0.99).

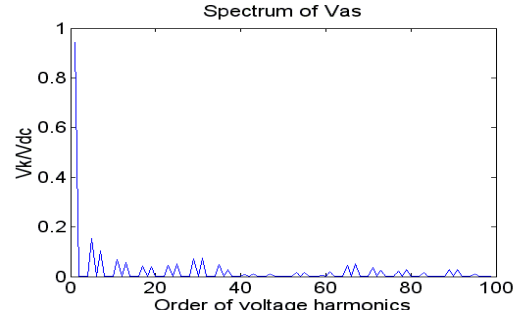

Fig. 22. Spectrum of the phase voltage V_{as} of the system with discontinuous synchronized PWM (F=49.5Hz, V_{dc2}=0.5V_{dc1}, F_{s1}=F_{s2}=1kHz).

The analysis of the phase voltage spectral composition in an asymmetrical dual inverter system with algorithms of synchronized PWM does not contain even harmonics or sub-harmonics in the zone of overmodulation (see Figs. 18, 20, 22).

VI. Dual-Inverter System on the Base of Neutral-Clamped Inverters without Zero Sequence Voltage

In order to increase the effectiveness of operation of an asymmetrical dual-inverter fed open-end winding motor drive, dual neutral-point-clamped inverters can also be used as elementary components of the dual-inverter topology. In particular, a specialized control scheme provides the elimination of zero sequence voltages in dual-inverter systems comprised of neutral-point-clamped inverters [14], [16], [18]. Fig. 23 presents the basic topology of a neutral-clamped inverter. Each of the three legs of the inverter consists of four power switches, four freewheeling diodes and two clamping diodes.

Fig. 24 shows the switching state vectors of the inverter. It is known, that the use of only seven of the vectors, V_1 - V_7, marked in Fig. 24 with the arrows and the corresponding vector number, provides elimination of zero sequence voltages [14]. A ternary switching variable (+, **0**, -) is defined for the switches of each one of the three phases:

\+ *if* S_1, S_2 *are* **ON** *and* S_3, S_4 *are* **OFF**;

0 *if* S_2, S_3 *are* **ON** *and* S_1, S_4 *are* **OFF**;

\- *if* S_3, S_4 *are* **ON** *and* S_1, S_2 *are* **OFF**.

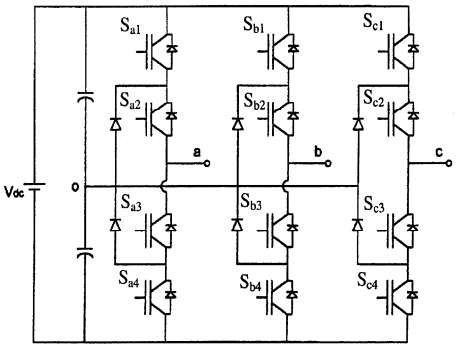

Fig. 23. Basic topology of three-phase neutral-point-clamped inverter.

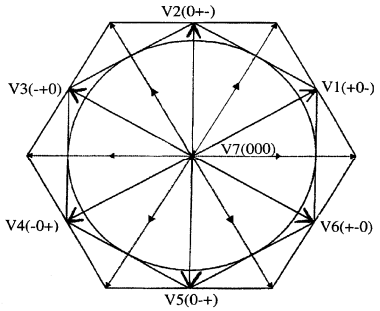

Fig. 24. Switching state vectors providing elimination of zero sequence voltage in system.

In this case the switching state sequences of the corresponding vectors are:

$$V_1(+0-);\ V_2(0+-);\ V_3(-+0);\ V_4(-0+);$$
$$V_5(0-+);\ V_6(+-0);\ V_7(000).$$

Two basic schemes of synchronized space-vector PWM have been elaborated for the control of neutral-point-clamped inverters in order to eliminate zero sequence voltages. These schemes can be applied to the control of an asymmetrical dual-inverter fed open winding system [14], [16]. In particular, Figs. 25-28 present pole voltages V_{a1o} and V_{a2o}, zero sequence voltage V_0, and phase voltage V_{as} (with its spectrum) in an asymmetrical (V_{dc2}=0.5V_{dc1}) dual-inverter system using neutral-clamped inverters. Discontinuous (DPWM, Figs. 25-26), and "direct-direct" (DDPWM, Figs. 27-28) schemes of synchronized PWM have been applied with scalar *V/F=const* control mode.

The fundamental and switching frequencies of each inverter (average switching frequency for discontinuous and "direct-direct" PWM) are correspondingly F=39Hz and F_s=1kHz, modulation indexes of the two neutral-clamped inverters are m_1=m_2=0.78, and ratio between the switching frequency and fundamental frequency is equal to 1000Hz/39Hz=25.6. Spectra of the phase voltage of this dual-inverter topology system do not contain undesirable even harmonics or sub-harmonics.

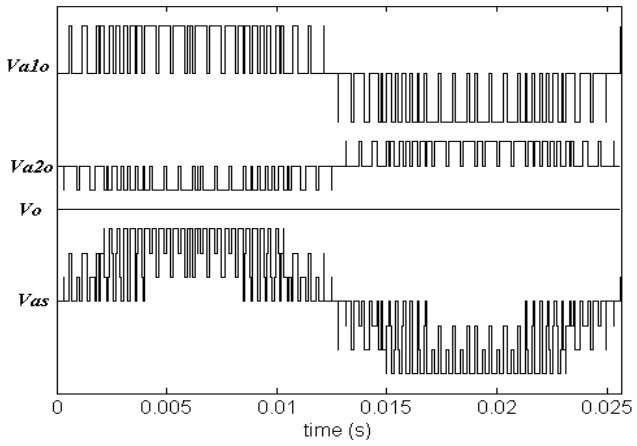

Fig. 25. Pole voltages V_{a1o}, V_{a2o}, zero sequence voltage V_0, and phase voltage V_{as} of dual-inverter fed system with neutral-clamped inverters with discontinuous synchronized PWM (F=39Hz, F_s=1kHz, m_1=m_2=0.78).

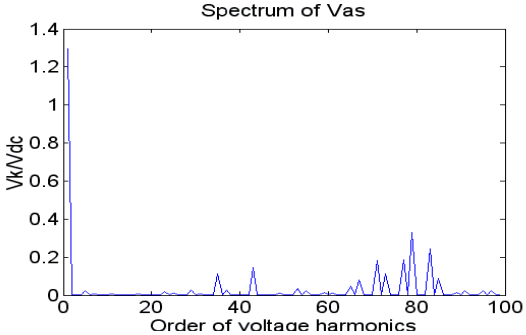

Fig. 26. Spectrum of the phase voltage V_{as} of system with neutral-clamped inverters with discontinuous synchronized PWM (F=39Hz, F_s=1kHz).

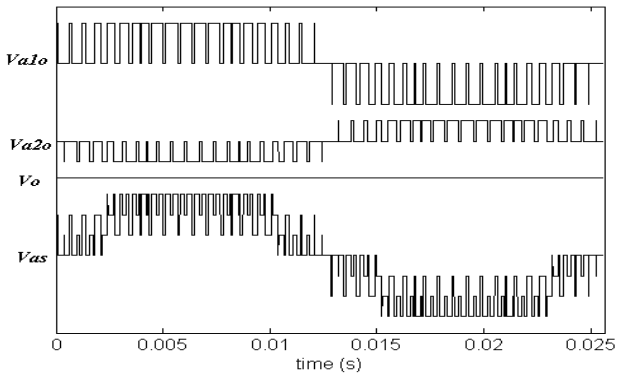

Fig. 27. Pole voltages V_{a1o}, V_{a2o}, zero sequence voltage V_0, and phase voltage V_{as} of dual-inverter fed system with neutral-clamped inverters with "direct-direct" synchronized PWM (F=39Hz, F_s=1kHz, m_1=m_2=0.78).

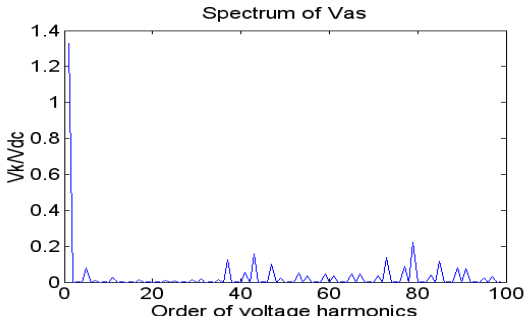

Fig. 28. Spectrum of the phase voltage V_{as} of system with neutral-clamped inverters with "direct-direct" synchronized PWM (F=39Hz, F_s=1kHz).

VII. Spectral Assessment of Phase Voltage Quality of Dual-Inverter System with Synchronized PWM

Voltage Weighted Total Harmonic Distortion (*WTHD*) factor is one of the most suitable criteria for analyzing the power quality in adjustable speed drive systems. Fig. 29 presents the calculation results of the *WTHD* factor

$$WTHD = (1/V_{as_1})(\sum_{k=2}^{1000}(V_{as_k}/k)^2)^{0.5}, \quad (12)$$

for phase voltage V_{as} as a function of modulation index m=m_1=m_2 of two inverters in an asymmetrical dual-inverter open-end winding drive system (V_{dc2}=0.5V_{dc1}). The results are shown in the case of two two-level inverters (with algorithms of continuous (CPWM) and discontinuous (DPWM) synchronized PWM), and also for neutral-point-clamped inverters, controlled by algorithms of "direct-direct" (DDPWM-NPC) and discontinuous (DPWM-NPC) schemes of synchronized modulation. Control mode of the drive system corresponds to standard scalar *V/F* control (linear modulation zone), and the average switching frequency of each inverter of the dual-inverter system is equal to F_s=1*kHz*.

The presented calculation results show that dual-inverter systems based on neutral-point-clamped inverters with specialized algorithms of synchronized PWM have better phase voltage spectral composition (in comparison to dual-inverter systems based on two-level inverters) in the zone of

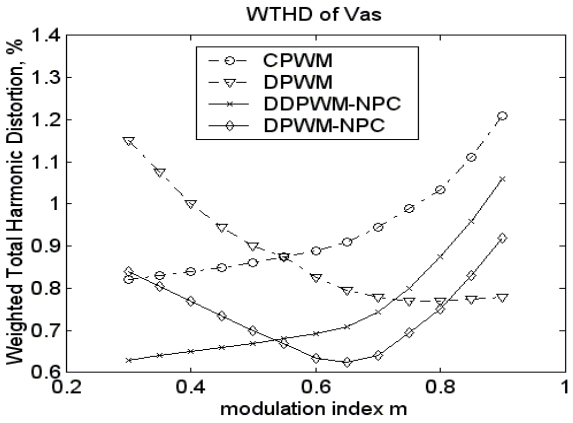

Fig. 29. Averaged *WTHD* factor of the phase voltage V_{as} versus modulation index m=m_1=m_2 for asymmetrical dual-inverter system (V_{dc2}=0.5V_{dc1}).

low and medium modulation indexes. It is also necessary to note that in the case of the dual-inverter topology based on two-level inverters, algorithms of discontinuous synchronized PWM provide better spectral composition of the phase voltage at higher fundamental frequencies (including the overmodulation zone).

VIII. Conclusion

Novel algorithms of space-vector-based synchronized PWM, disseminated for the control of asymmetrical dual-inverter fed open-end winding motor systems based on two voltage source inverters, supplied by two isolated dc sources (V_{dc2}=0.5V_{dc1}), allow continuous symmetry of phase voltage waveforms during the whole control range and for any operating conditions. Spectra of the phase voltage of dual-inverter drives with algorithms of synchronized PWM do not contain even harmonics or sub-harmonics, which is especially important for systems with increased power rating, including medium-power and high-power traction systems and propulsion systems. In particular:

1. Algorithms of synchronized PWM provide phase voltage symmetry for any ratio (integral or fractional) between the switching frequency and fundamental frequency of each inverter of dual-inverter systems (see the corresponding Figs. 5-8, illustrating the operation of the system with algorithms of continuous (Figs. 5-6) and discontinuous (Figs. 7-8) synchronized PWM. Frequency ratio is equal to F_s/F = 1000*Hz*/39*Hz* = 25.6 in this case).
2. Algorithms of synchronized PWM provide phase voltage symmetry in dual-inverter systems with different switching frequencies of the two inverters (see the corresponding Figs. 9-12, illustrating the operation of the system with algorithms of continuous (Figs. 9-10) and discontinuous (Figs. 11-12) synchronized PWM. Frequency ratio of the first inverter is equal to F_s/F=1000*Hz*/39*Hz*=25.6, and frequency ratio of the second inverter is equal to F_s/F=2000*Hz*/39*Hz*=51.2 in this case).

3. Algorithms of synchronized PWM provide phase voltage symmetry of dual-inverter system with different voltage ratios of two isolated dc-sources (see the corresponding Figs. 13-16, illustrating the operation of the system with algorithms of continuous (Figs. 13-14) and discontinuous (Figs. 15-16) synchronized PWM. Voltage ratio is equal to V_{dc2}/V_{dc1}=0.7, frequency ratio of the first inverter is equal to F_s/F=1000*Hz*/32*Hz*=31.25, and frequency ratio of the second inverter is equal to F_s/F= 1430*Hz*/32*Hz*=44.7 in this case).
4. Algorithms of synchronized PWM provide phase voltage symmetry of dual-inverter systems inside the overmodulation zone (see the corresponding Figs. 17-20, illustrating the operation of the system with algorithms of discontinuous synchronized PWM in the first (Figs. 17-18) and the second (Figs. 19-20) parts of the zone of overmodulation. Frequency ratio of the first inverter is equal to F_s/F =1000*Hz*/47*Hz*=21.3 and to F_s/F=1000*Hz*/ 49.5*Hz* =20.2, and frequency ratio of the second inverter is equal to F_s/F=2000*Hz*/47*Hz*=42.6 and to F_s/F= 2000*Hz*/49.5*Hz*=40.4 in these cases).
5. Algorithms of synchronized PWM provide phase voltage symmetry for dual-inverter systems based on two neutral-point-clamped inverters with synchronized PWM for any ratio (integral or fractional) between the switching frequency and fundamental frequency of each inverter of the system (see the corresponding Figs. 25-28, illustrating the operation of the system with specialized algorithms of discontinuous (Figs. 25-26) and "direct-direct" (Figs. 27-28) synchronized PWM. Frequency ratio is equal to F_s/F=1000*Hz*/ 39*Hz*=25.6 in this case).
6. Dual-inverter system on the base of neutral-point-clamped inverters with specialized algorithms of synchronized PWM have better phase voltage spectral composition (in comparison to dual-inverter systems based on two-level inverters) in the zone of low and medium modulation indexes of the two inverters.

The analyzed configurations of asymmetrical dual-inverter fed open-end winding motor drives controlled by algorithms of synchronized PWM can also be used as basic components of different multiphase multi-inverter systems, such as the quad inverter ac motor drive proposed in [19]-[22].

REFERENCES

[l] H. Stemmler, and P. Guggenbach, "Configurations of high power voltage source inverter drives", *Proc. of the European Power Electronics Conf*., pp. 7-12, 1993.

[2] H. Stemmler, "High-power industrial drives", *IEEE Proc*., vol. 82, no. 8, pp. 1266-1286, 1994.

[3] K.A. Corzine, S.D. Sudhoff, and C.A. Whitcomb, "Performance characteristics of a cascaded two-level converter", *IEEE Trans. on Energy Conversion*, vol.14, no.3, pp.433-439, 1999.

[4] G. Grandi, C. Rossi, A. Lega, D. Casadei: "*Power balancing of a multilevel converter with two insulated supplies for three-phase six-wire loads*". 11th European Conference on Power Electronics and Applications, EPE 2005, Dresden (D), September 11-14, 2005.

[5] G. Grandi, C. Rossi, A. Lega, D. Casadei: "*Multilevel operation of a dual two-level inverter with power balancing capability*", 41st IEEE-IAS Annual Meeting, Tampa, Florida (USA), Oct. 8 - 12, 2006.

[6] D. Casadei, G. Grandi, A. Lega, C. Rossi, L. Zarri: "*Switching technique for dual-two level inverter supplied by two separate sources*", Applied Power Electronics Conference and Exposition, APEC, Anaheim, California (USA), Feb. 25 - Mar. 1, 2007, pp.1522-1528.

[7] D. Casadei, G. Grandi, A. Lega, C. Rossi: "*Multilevel Operation and Input Power Balancing for a Dual Two-Level Inverter with Insulated dc Sources*", IEEE Trans. on Industry Applications, vol. 44, No. 6, Nov/Dec 2008, pp. 1815-1824.

[8] G. Grandi, D. Ostojic, "Dual inverter space vector modulation with power balancing capability", *in Proc. IEEE Reg.8 Conf., EUROCON'09,* St. Petersburg (RUS), pp. 721–728, 18–23 May 2009.

[9] B.V. Reddy, V.T. Somasekhar, and Y. Kalyan, "Decoupled space-vector PWM strategies for a four-level asymmetrical open-end winding induction motor drive with waveform symmetries," *IEEE Trans. on Industrial Electronics*, vol. 58, no. 11, pp. 5130-5141, 2011.

[10] J. Holtz, "Pulsewidth modulation – a survey," *IEEE Trans. on Industrial Electronics,* vol. 39, no. 5. pp. 410-420, 1992.

[11] N. Mohan, T.M. Undeland, and W.P. Robbins, *Power Electronics, 3rd ed*. John Wiley & Sons, 2003.

[12] R.K. Jardan, P. Stumpf, P. Bartal, Z. Varga, and I. Nagy, "A novel approach in studying the effects of subharmonics on ultrahigh speed AC motor drives," *IEEE Trans. on Industrial Electronics*, vol. 58, no. 4, pp. 1274-1281, 2011.

[13] V. Oleschuk, F. Blaabjerg, and B.K. Bose, "Analysis and comparison of algebraic and trigonometric methods of synchronous PWM for inverter drives," *Proc. of the IEEE Power Electronics Specialists Conf.,* pp. 1439-1444, 2002.

[14] V. Oleschuk, and F. Blaabjerg, "Three-level inverters with common-mode voltage cancellation based on synchronous pulsewidth modulation" *Proc. of the IEEE Power Electronics Specialists Conf.,* pp. 863-868, 2002.

[15] V. Oleschuk, V. Ermuratski, and E.M. Chekhet, "Drive converters with synchronized pulsewidth modulation during overmodulation", *Proc. of the IEEE Int'l Symp. on Ind. Electronics*, pp.1339-1344, 2004.

[16] V. Oleschuk, F. Profumo, A. Tenconi, R. Bojoi, and A.M. Stankovic, "Cascaded three-level inverters with synchronized space-vector modulation,", *Proc. of the IEEE Ind. Application Society Conf.,* pp. 595-602, 2006.

[17] V. Oleschuk, and G. Griva, "Synchronized space-vector modulation for six-phase automotive drive with controlled switching frequency," *Intl. Review of Electrical Engineering*, vol. 4, no. 1, pp. 50-56, 2009.

[18] V. Oleschuk, G. Griva, and F. Spertino, "Dual neutral-point-clamped converters with synchronized PWM for photovoltaic installations," *International Review of Electrical Engineering*, vol. 5, no. 1(A), pp. 55-63, 2010.

[19] G. Grandi, A. Tani, P. Sanjeevkumar, and D. Ostojic, "Multi-phase multi-level AC motor drive based on four three-phase two-level inverters," *Proc. IEEE Int'l Symp. on Power Electronics, Electrical Drives, Automation and Motion, SPPEDAM'10*, pp. 1768-1775, 2010.

[20] G. Grandi, P. Sanjeevikumar, D. Ostojic, C. Rossi, "Quad Inverter Configuration for Multi-Phase Multi-Level AC Motor Drives," IEEE Intl. Conf. on Computational Technologies in Electrical and Electronics Engineering, SIBIRCON'10, Irkutsk (RU), July 11–15, 2010.

[21] V. Oleschuk, G. Grandi, and P. Sanjeevikumar, "Simulation of processes in dual three-phase system on the base of four inverters with synchronized modulation," *Advances in Power Electronics*, Article ID 581306, vol. 2011 (2011).

[22] G. Grandi, P. Sanjeevikumar, D. Casadei, "Preliminary hardware implementation of a six-phase quad-inverter induction motor drive," *in Proc. of European Power Electronic and Application Conf., EPE'11,* Birmingham (UK), pp. 1–9, 30 Aug.–1 Sept. 2011.